



BELLE Preprint 2004-27
 KEK Preprint 2004-54
 14 August 2019

Measurement of masses and branching ratios of Ξ_c^+ and Ξ_c^0 baryons

Belle Collaboration

T. Lesiak ^{ad}, K. Abe ^j, K. Abe ^{at}, I. Adachi ^j, H. Aihara ^{av},
 Y. Asano ^{bb}, S. Bahinipati ^f, A. M. Bakich ^{aq}, A. Bay ^t,
 U. Bitenc ^o, I. Bizjak ^o, A. Bondar ^b, A. Bozek ^{ad}, M. Bračko ^{v,o},
 J. Brodzicka ^{ad}, T. E. Browder ⁱ, Y. Chao ^{ac}, A. Chen ^z,
 B. G. Cheon ^d, R. Chistov ⁿ, S.-K. Choi ^h, Y. Choi ^{ap},
 A. Chuvikov ^{ak}, S. Cole ^{aq}, J. Dalseno ^w, M. Danilov ⁿ,
 M. Dash ^{bd}, S. Eidelman ^b, V. Eiges ⁿ, S. Fratina ^o,
 N. Gabyshev ^b, A. Garmash ^{ak}, T. Gershon ^j, A. Go ^z,
 G. Gokhroo ^{ar}, J. Haba ^j, K. Hayasaka ^x, M. Hazumi ^j, L. Hinz ^t,
 Y. Hoshi ^{at}, S. Hou ^z, W.-S. Hou ^{ac}, T. Iijima ^x, A. Imoto ^y,
 K. Inami ^x, A. Ishikawa ^j, R. Itoh ^j, M. Iwasaki ^{av}, J. H. Kang ^{be},
 J. S. Kang ^q, N. Katayama ^j, H. Kawai ^c, T. Kawasaki ^{af},
 H. R. Khan ^{aw}, K. Kinoshita ^f, S. Korpar ^{v,o}, P. Krovovny ^b,
 S. Kumar ^{ai}, C. C. Kuo ^z, A. Kuzmin ^b, Y.-J. Kwon ^{be},
 J. S. Lange ^g, G. Leder ^m, S.-W. Lin ^{ac}, J. MacNaughton ^m,
 G. Majumder ^{ar}, F. Mandl ^m, T. Matsumoto ^{ay}, A. Matyja ^{ad},
 W. Mitaroff ^m, H. Miyata ^{af}, G. R. Moloney ^w, T. Nagamine ^{au},
 Y. Nagasaka ^k, T. Nakadaira ^{av}, E. Nakano ^{ag}, M. Nakao ^j,
 Z. Natkaniec ^{ad}, S. Nishida ^j, O. Nitoh ^{az}, S. Ogawa ^{as},
 T. Ohshima ^x, T. Okabe ^x, S. Okuno ^p, S. L. Olsen ⁱ,
 W. Ostrowicz ^{ad}, H. Ozaki ^j, H. Park ^s, K. S. Park ^{ap},

N. Parslow^{aq}, L. S. Peak^{aq}, L. E. Piilonen^{bd}, M. Rozanska^{ad},
H. Sagawa^j, Y. Sakai^j, N. Sato^x, T. Schietinger^t,
O. Schneider^t, S. Semenovⁿ, H. Shibuya^{as}, A. Somov^f,
N. Soni^{ai}, R. Stamen^j, S. Stanič^{bb,†}, M. Starič^o,
T. Sumiyoshi^{ay}, K. Tamai^j, N. Tamura^{af}, M. Tanaka^j,
Y. Teramoto^{ag}, T. Tsuboyama^j, T. Tsukamoto^j, S. Uehara^j,
K. Ueno^{ac}, S. Uno^j, Y. Ushiroda^j, G. Varnerⁱ, K. E. Varvell^{aq},
S. Villa^t, C. C. Wang^{ac}, C. H. Wang^{ab}, Q. L. Xie^ℓ,
B. D. Yabsley^{bd}, A. Yamaguchi^{au}, Y. Yamashita^{ae}, J. Ying^{aj},
Y. Yusa^{au}, C. C. Zhang^ℓ, J. Zhang^j, L. M. Zhang^{an},
Z. P. Zhang^{an}, V. Zhilich^b, and D. Žontar^{u,o}

^a*Aomori University, Aomori, Japan*

^b*Budker Institute of Nuclear Physics, Novosibirsk, Russia*

^c*Chiba University, Chiba, Japan*

^d*Chonnam National University, Kwangju, South Korea*

^e*Chuo University, Tokyo, Japan*

^f*University of Cincinnati, Cincinnati, OH, USA*

^g*University of Frankfurt, Frankfurt, Germany*

^h*Gyeongsang National University, Chinju, South Korea*

ⁱ*University of Hawaii, Honolulu, HI, USA*

^j*High Energy Accelerator Research Organization (KEK), Tsukuba, Japan*

^k*Hiroshima Institute of Technology, Hiroshima, Japan*

^l*Institute of High Energy Physics, Chinese Academy of Sciences, Beijing, PR China*

^m*Institute of High Energy Physics, Vienna, Austria*

ⁿ*Institute for Theoretical and Experimental Physics, Moscow, Russia*

^o*J. Stefan Institute, Ljubljana, Slovenia*

^p*Kanagawa University, Yokohama, Japan*

^q*Korea University, Seoul, South Korea*

^r*Kyoto University, Kyoto, Japan*

^s*Kyungpook National University, Taegu, South Korea*

^t*Swiss Federal Institute of Technology of Lausanne, EPFL, Lausanne*

^u*University of Ljubljana, Ljubljana, Slovenia*

^v*University of Maribor, Maribor, Slovenia*

^w*University of Melbourne, Victoria, Australia*

^x*Nagoya University, Nagoya, Japan*

^y*Nara Women's University, Nara, Japan*

^z*National Central University, Chung-li, Taiwan*

^{aa}*National Kaohsiung Normal University, Kaohsiung, Taiwan*

^{ab}*National United University, Miao Li, Taiwan*

^{ac}*Department of Physics, National Taiwan University, Taipei, Taiwan*

^{ad}*H. Niewodniczanski Institute of Nuclear Physics, Krakow, Poland*

^{ae}*Nihon Dental College, Niigata, Japan*

^{af}*Niigata University, Niigata, Japan*

^{ag}*Osaka City University, Osaka, Japan*

^{ah}*Osaka University, Osaka, Japan*

^{ai}*Panjab University, Chandigarh, India*

^{aj}*Peking University, Beijing, PR China*

^{ak}*Princeton University, Princeton, NJ, USA*

^{al}*RIKEN BNL Research Center, Brookhaven, NY, USA*

^{am}*Saga University, Saga, Japan*

^{an}*University of Science and Technology of China, Hefei, PR China*

^{ao}*Seoul National University, Seoul, South Korea*

^{ap}*Sungkyunkwan University, Suwon, South Korea*

^{aq}*University of Sydney, Sydney, NSW, Australia*

^{ar}*Tata Institute of Fundamental Research, Bombay, India*

^{as}*Toho University, Funabashi, Japan*

^{at}*Tohoku Gakuin University, Tagajo, Japan*

^{au}*Tohoku University, Sendai, Japan*

^{av}*Department of Physics, University of Tokyo, Tokyo, Japan*

^{aw}*Tokyo Institute of Technology, Tokyo, Japan*

^{ay}*Tokyo Metropolitan University, Tokyo, Japan*

^{az}*Tokyo University of Agriculture and Technology, Tokyo, Japan*

^{ba}*Toyama National College of Maritime Technology, Toyama, Japan*

^{bb}*University of Tsukuba, Tsukuba, Japan*

^{bc}*Utkal University, Bhubaneswar, India*

^{bd}*Virginia Polytechnic Institute and State University, Blacksburg, VA, USA*

^{be}*Yonsei University, Seoul, South Korea*

[†] on leave from Nova Gorica Polytechnic, Nova Gorica, Slovenia

Abstract

We report a measurement of the Ξ_c^+ and Ξ_c^0 baryon masses, and the branching ratios for various Ξ_c decays, using 140 fb^{-1} of data collected by the Belle experiment at the KEKB e^+e^- collider. The mass splitting $m_{\Xi_c^0} - m_{\Xi_c^+}$ is found to be $2.9 \pm 0.5\text{ MeV}/c^2$; this measurement is three times as precise as the current world average. We measure the branching ratios $\Gamma(\Xi_c^+ \rightarrow \Lambda K\pi\pi)/\Gamma(\Xi_c^+ \rightarrow \Xi\pi\pi) = 0.32 \pm 0.03 \pm 0.02$ and $\Gamma(\Xi_c^0 \rightarrow pKK\pi)/\Gamma(\Xi_c^0 \rightarrow \Xi\pi) = 0.33 \pm 0.03 \pm 0.03$, with improved precision, and measure $\Gamma(\Xi_c^+ \rightarrow pK_S^0 K_S^0)/\Gamma(\Xi_c^+ \rightarrow \Xi\pi\pi) = 0.087 \pm 0.016 \pm 0.014$, $\Gamma(\Xi_c^0 \rightarrow \Lambda K\pi)/\Gamma(\Xi_c^0 \rightarrow \Xi\pi) = 1.07 \pm 0.12 \pm 0.07$ and $\Gamma(\Xi_c^0 \rightarrow \Lambda K_S^0)/\Gamma(\Xi_c^0 \rightarrow \Xi\pi) = 0.21 \pm 0.02 \pm 0.02$ for the first time. In Ξ_c^0 decays to the $pK^-K^-\pi^+$ final state, we find evidence for the process $\Xi_c^0 \rightarrow pK^-\bar{K}^*(892)^0$ and measure the fraction of decays via this process to be $0.51 \pm 0.03 \pm 0.01$.

Author Keywords Charmed baryon; W-exchange

PACS classification codes 13.30Eg; 14.20Lq

1 Introduction

Despite significant progress in experimental studies of charmed baryons, the properties of the Ξ_c baryons are still poorly known. The current world average masses are $(2466.3 \pm 1.4)\text{ MeV}/c^2$ for the Ξ_c^+ and $(2471.8 \pm 1.4)\text{ MeV}/c^2$ for the Ξ_c^0 , and the precision on the mass splitting is comparable, $\pm 1.8\text{ MeV}/c^2$ [1]. Among the exclusive decays reported so far, only the observations by the CLEO [2,3,4] and FOCUS [5,6] collaborations are based on data samples of more than 100 events. No absolute branching fractions have been measured, and branching ratios relative to the ‘reference modes’ $\Xi_c^+ \rightarrow \Xi^-\pi^+\pi^+$ and $\Xi_c^0 \rightarrow \Xi^-\pi^+$ have been determined with a typical precision of only 30%.

This Letter presents the results of a study of exclusive Ξ_c decays in e^+e^- continuum production, with ≈ 3000 observed events in the reference modes. Branching ratios for Ξ_c^+ decays to the $\Lambda K^-\pi^+\pi^+$ and $pK_S^0 K_S^0$ final states,* and for Ξ_c^0 decays to $\Lambda K^-\pi^+$, ΛK_S^0 and $pK^-K^-\pi^+$, have been measured with a typical precision of $\approx 15\%$. The large reconstructed samples also allow precise measurements of the Ξ_c masses, and in particular the mass splitting between the neutral and charged states.

The decay $\Xi_c^0 \rightarrow \Lambda K_S^0$ is of particular interest, as it can occur only via the poorly known W -boson-exchange process (Fig. 1(a)) or the internal-spectator diagram (Fig. 1(b)), in the absence of final state interactions. Theoretical predictions for this mode are based, for example, on a symmetric-quark-model approach [7,8], and span a range of branching fractions from 0.4% to 0.7% [9,10]; the fraction for the reference decay $\Xi_c \rightarrow \Xi^-\pi^+$ is predicted to lie between 0.9% and 2%.

* Charge conjugate modes are included everywhere, unless otherwise specified.

This paper is organized as follows. Section 2 describes the detector and data sample, and Section 3 describes the reconstruction of Ξ_c baryons. The remaining sections present our determination of the Ξ_c masses (Section 4) and branching fractions (Section 5). Section 5.1 presents a study of the resonant substructure of the $\Xi_c^0 \rightarrow pK^-K^-\pi^+$ decay, improving on the precision of the recent CLEO measurement [4].

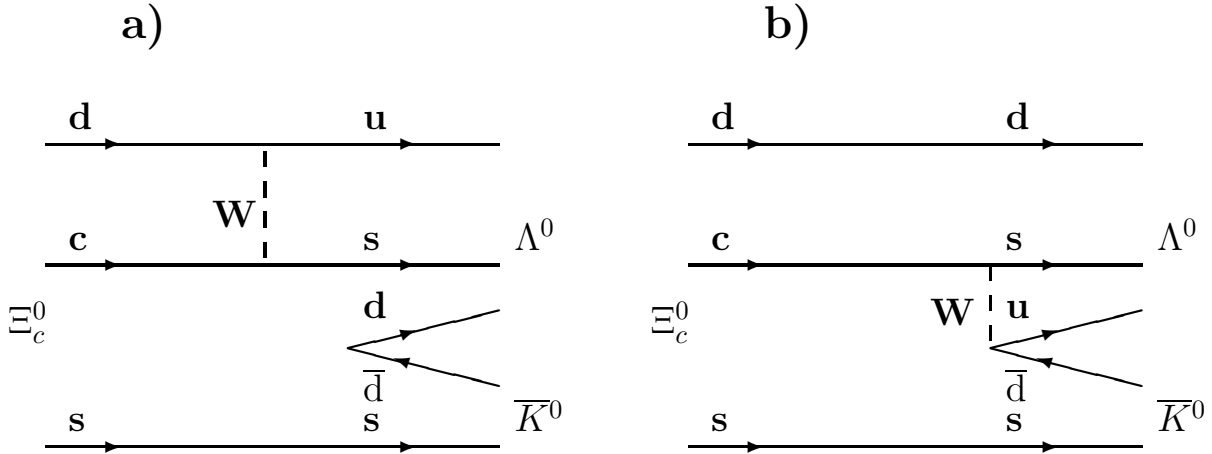


Fig. 1. Feynman diagrams for the process $\Xi_c^0 \rightarrow \Lambda K_S^0$: (a) W exchange and (b) internal spectator.

2 Detector and data sample

The data used for this study were collected on the $\Upsilon(4S)$ resonance using the Belle detector at the KEKB asymmetric e^+e^- collider [11]. The integrated luminosity of the data sample is 140 fb^{-1} .

The Belle detector is a large-solid-angle magnetic spectrometer that consists of a three-layer silicon vertex detector (SVD), a 50-layer central drift chamber (CDC), an array of aerogel threshold Čerenkov counters (ACC), a barrel-like arrangement of time-of-flight scintillation counters (TOF), and an electromagnetic calorimeter comprised of CsI(Tl) crystals (ECL) located inside a super-conducting solenoid coil that provides a 1.5 T magnetic field. An iron flux-return located outside of the coil is instrumented to detect K_L^0 mesons and to identify muons (KLM). A detailed description of the Belle detector can be found elsewhere [12].

3 Reconstruction

Reconstruction of Ξ_c decays for this analysis proceeds in three steps: reconstruction of tracks and their identification as protons, kaons or pions; combination of tracks to reconstruct K_S^0 mesons and Λ and Ξ^- hyperons; and the selection of Ξ_c candidates from combinations of tracks, K_S^0 's and hyperons. The method for each step is described in the following sections in turn.

3.1 Track reconstruction and identification

Charged tracks are reconstructed from hits in the CDC using a Kalman filter [13], and matched to hits in the SVD where present. Quality criteria are then applied. Excepting those tracks used to form K_S^0 , Λ and Ξ^- candidates, all tracks are required to have impact parameters relative to the interaction point (IP) of less than 0.5 cm in the $r - \phi$ plane, and 5 cm in the z direction. (The z -axis is oriented opposite to the direction of the e^+ beam, along the symmetry axis of the detector.) The transverse momentum of each track is required to exceed $0.1 \text{ GeV}/c$, in order to reduce the low momentum combinatorial background.

Identification of tracks is based on information from the CDC (energy loss dE/dx), TOF and ACC, combined to form likelihoods $\mathcal{L}(p)$, $\mathcal{L}(K)$ and $\mathcal{L}(\pi)$ for the proton, kaon and pion hypotheses respectively. These likelihoods are combined to form ratios $\mathcal{P}(K/\pi) = \mathcal{L}(K)/(\mathcal{L}(K) + \mathcal{L}(\pi))$ and $\mathcal{P}(p/K) = \mathcal{L}(p)/(\mathcal{L}(p) + \mathcal{L}(K))$, spanning the range from zero to one, which are then used to select track samples. Kaon candidates are required to satisfy $\mathcal{P}(K/\pi) > 0.9$ and $\mathcal{P}(p/K) < 0.98$; the second criterion is to veto protons. This selection has an efficiency of 80% and a fake rate of 3.8% (π fakes K). Protons are required to satisfy $\mathcal{P}(p/K) > 0.9$. Pion candidates, except those coming from the decay of the Λ hyperon, should satisfy both a proton and a kaon veto: $\mathcal{P}(p/K) < 0.98$ and $\mathcal{P}(K/\pi) < 0.98$.

Electrons are identified using a similar likelihood ratio $\mathcal{P}_e = \mathcal{L}_e/(\mathcal{L}_e + \mathcal{L}_{\text{non-}e})$, based on a combination of dE/dx measurements in the CDC, the response of the ACC, and E/p , where p is the momentum of the track and E the energy of the associated cluster in the ECL. All tracks with $\mathcal{P}_e > 0.98$ are assumed to be electrons, and removed from the proton, kaon and pion samples.

3.2 Reconstruction of Λ , K_S^0 , and Ξ^-

We reconstruct Λ hyperons in the $\Lambda \rightarrow p\pi$ decay mode, requiring the proton track to satisfy $\mathcal{P}(p/K) > 0.1$, and fitting the p and π tracks to a common vertex. The $\chi^2/n.d.f.$ of the vertex should not exceed 25, and the difference in the z -coordinate between the proton and pion at the vertex is required to be less than 2 cm. Due to the large $c\tau$ factor for Λ hyperons (7.89 cm), we demand that the distance between the decay vertex and the IP in the $r - \phi$ plane be greater than 1 cm. The invariant mass of the proton-pion pair is required to be within $2.4 \text{ MeV}/c^2$ (≈ 2.5 standard deviations) of the nominal Λ mass.

K_S^0 mesons are reconstructed using pairs of charged tracks that have an invariant mass within $6 \text{ MeV}/c^2$ (2.5 standard deviations) of the nominal K_S^0 mass, and a well reconstructed vertex displaced from the IP by at least 5 mm.

We reconstruct Ξ^- hyperons in the decay mode $\Xi^- \rightarrow \Lambda\pi^-$. The Λ and π candidates are fitted to a common vertex, whose $\chi^2/n.d.f.$ is required to be at most 25. The distance between the Ξ^- vertex position and interaction point in the $r - \phi$ plane should be at least 5 mm, and less than the corresponding distance between the IP and the Λ vertex. The invariant mass of the $\Lambda\pi^-$ pair is required to be within $7.5 \text{ MeV}/c^2$ of the nominal value (≈ 2.5 standard deviations).

3.3 Reconstruction of Ξ_c^+ and Ξ_c^0

Charged hadrons, K_S^0 mesons and Λ and Ξ^- hyperons are combined to form candidates for three decays of the charged Ξ_c ,

$$\Xi_c^+ \rightarrow \Xi^- \pi^+ \pi^+ \quad (1)$$

$$\Xi_c^+ \rightarrow \Lambda K^- \pi^+ \pi^+ \quad (2)$$

$$\Xi_c^+ \rightarrow p K_S^0 K_S^0 \quad (3)$$

and four decays of the neutral state,

$$\Xi_c^0 \rightarrow \Xi^- \pi^+ \quad (4)$$

$$\Xi_c^0 \rightarrow \Lambda K^- \pi^+ \quad (5)$$

$$\Xi_c^0 \rightarrow \Lambda K_S^0 \quad (6)$$

$$\Xi_c^0 \rightarrow p K^- K^- \pi^+. \quad (7)$$

Combinatorial and $B\bar{B}$ backgrounds are suppressed by requiring that the momentum of the Ξ_c candidate in the e^+e^- center-of-mass system exceed 2.5 GeV/ c . The decay products are fitted to a common vertex, and a goodness-of-fit criterion is applied: for decays (2), (3), (5) and (6), which contain a V^0 (Λ or K_S^0) in the final state, we require $\chi^2/n.d.f. < 10$; for the remaining decays, we require $\chi^2/n.d.f. < 50$.

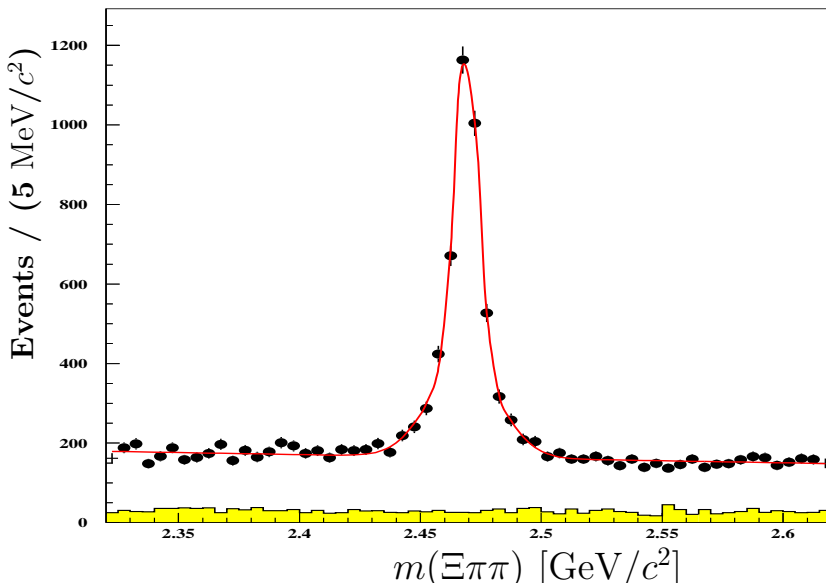


Fig. 2. Invariant mass distribution of selected $\Xi^- \rightarrow \Lambda \pi^- \pi^+ \pi^+$ combinations (points), the fit described in the text (curve), and wrong-sign combinations ($\Lambda^- \pi^- \pi^+ \pi^+$) (shaded).

A clear Ξ_c baryon signal is observed in the invariant mass distributions of each of the decays studied (Figs. 2–8). In particular, we observe the first evidence for the decay $\Xi_c^+ \rightarrow p K_S^0 K_S^0$. For each decay mode, we extract the signal yield and the Ξ_c mass and width from a fit to the distribution.

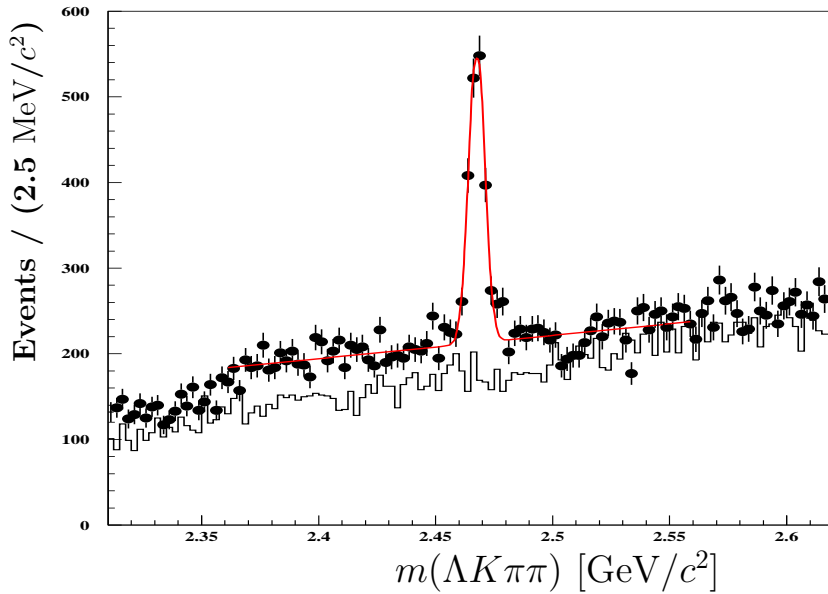


Fig. 3. Invariant mass distribution of selected $\Lambda K^- \pi^+ \pi^+$ combinations (points), the fit described in the text (curve), and wrong-sign combinations $\Lambda K^+ \pi^- \pi^-$ (histogram).

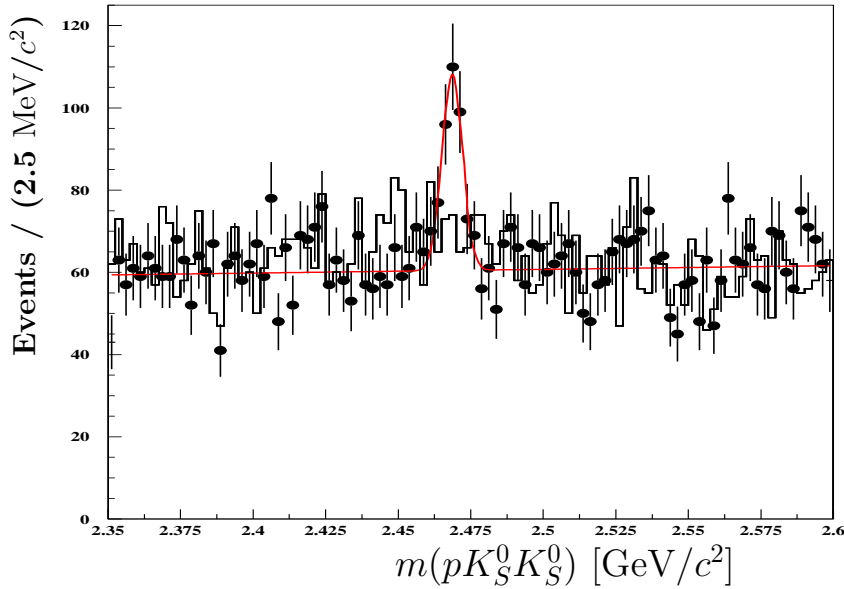


Fig. 4. Invariant mass distribution of selected $p K_S^0 K_S^0$ combinations (points), the fit described in the text (curve), and $p K_S^0 K_S^0$ combinations from the $K_S^0 \rightarrow \pi^+ \pi^-$ mass sideband $11 \text{ MeV}/c^2 < |m(\pi^+ \pi^-) - 497.7 \text{ MeV}/c^2| < 17 \text{ MeV}/c^2$ (histogram).

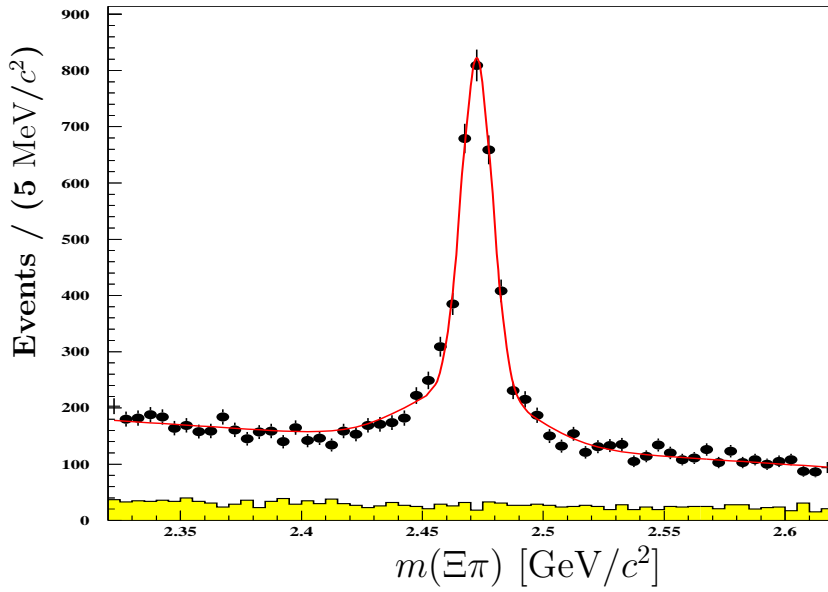


Fig. 5. Invariant mass distribution of selected $\Xi^- \rightarrow \Lambda^- \pi^+$ combinations (points), the fit described in the text (curve), and wrong-sign combinations $(\bar{\Lambda} \pi^-) \pi^+$ (shaded).

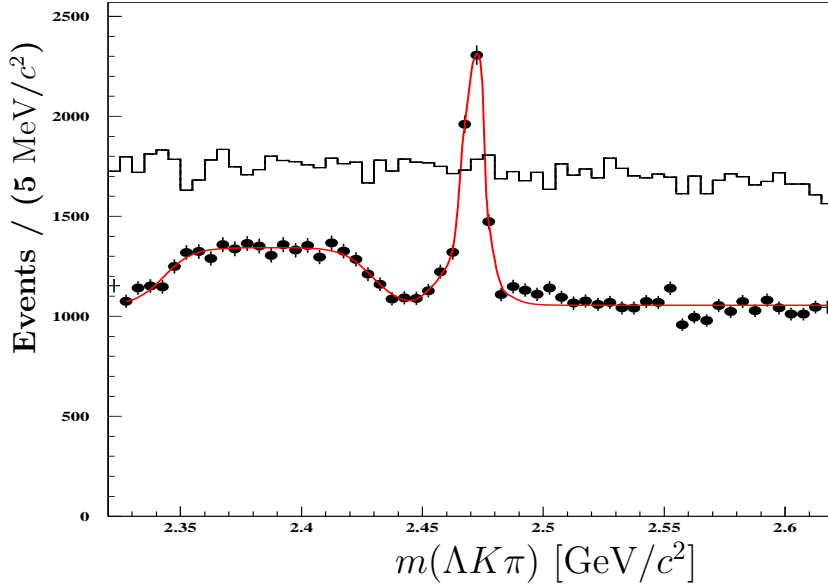


Fig. 6. Invariant mass distribution of selected $\Lambda K^- \pi^+$ combinations (points), the fit described in the text (curve), and wrong-sign combinations $\Lambda K^+ \pi^-$ (histogram). The structure centered at $2.37 \text{ GeV}/c^2$ is discussed in the text.

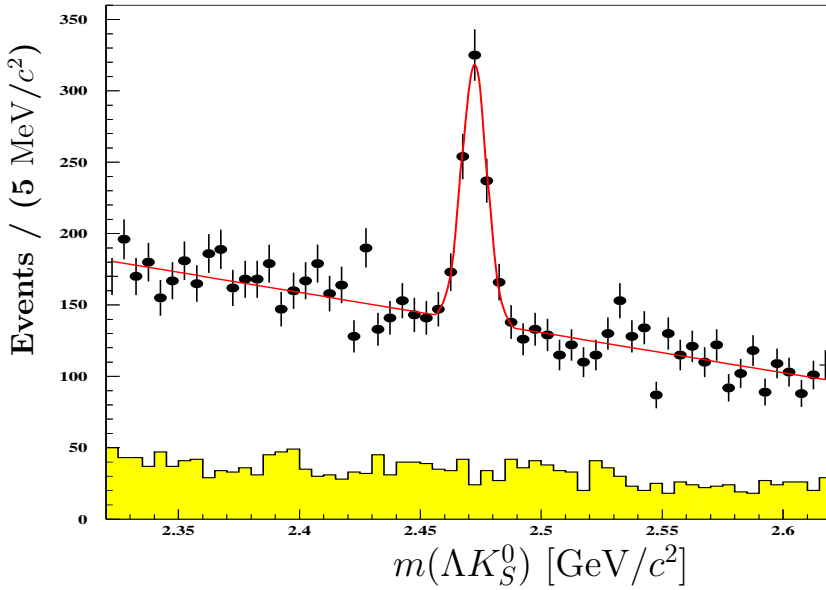


Fig. 7. Invariant mass distribution of selected ΛK_S^0 combinations (points), the fit described in the text (curve), and ΛK_S^0 combinations from the $K_S^0 \rightarrow \pi^+\pi^-$ mass sideband $11 \text{ MeV}/c^2 < |m(\pi^+\pi^-) - 497.7 \text{ MeV}/c^2| < 17 \text{ MeV}/c^2$ (shaded).

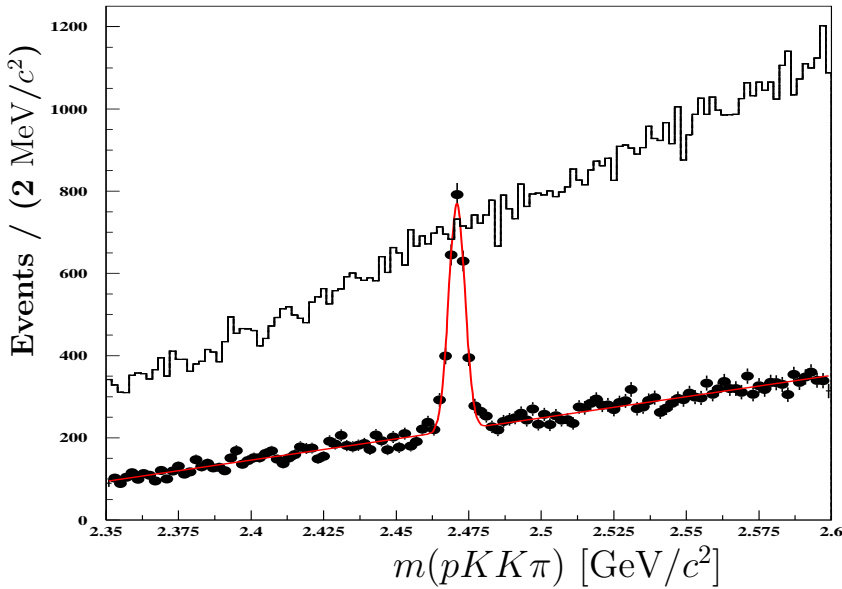


Fig. 8. Invariant mass distribution of selected $pK^-K^-\pi^+$ combinations (points), the fit described in the text (curve), and wrong-sign combinations $pK^-K^+\pi^-$ (histogram).

For the decays $\Xi_c^+ \rightarrow \Xi^- \pi^+ \pi^+$, $\Xi_c^0 \rightarrow \Xi^- \pi^+$ and $\Xi_c^0 \rightarrow \Lambda K^- \pi^+$, we use a double Gaussian for the signal (the second Gaussian is required to account for the tails in the signal shape) and a linear background function. In each case, the means of both Gaussians coincide within the errors of the fits. The broad enhancement in the $M(\Lambda K\pi)$ distribution (Fig. 6), below the Ξ_c mass, is assumed to be due to $\Xi(2370) \rightarrow \Lambda K\pi$ decays with an admixture of a kinematic reflection; it is represented with the function $f(x) = 1/(1 + \exp((|x - \bar{x}| - \sigma_x)/z))$ [14], where x is the $\Lambda K\pi$ invariant mass and \bar{x} , σ_x and z are parameters allowed to float in the fit. The mass and width of this structure are compatible with the parameters of the $\Xi(2370)$ resonance [1].

For the decays $\Xi_c^+ \rightarrow \Lambda K^- \pi^+ \pi^+$, $\Xi_c^+ \rightarrow p K_S^0 K_S^0$, $\Xi_c^0 \rightarrow \Lambda K_S^0$ and $\Xi_c^0 \rightarrow p K^- K^- \pi^+$, we use a single Gaussian for the signal and a linear background function. In each case the Ξ_c width is found to be compatible with the value from Monte Carlo simulation.

Figures 2, 3, 5, 6 and 8 also show the distribution of “wrong-sign” combinations, for which charge-conjugate states are used for certain particles. Figures 4 and 7 include the invariant mass spectrum for Ξ_c candidates taken from $K_S^0 \rightarrow \pi^+ \pi^-$ mass sidebands. These distributions are structureless and provide a cross-check for the shape of the combinatorial background in the Ξ_c sample.

The fit results are summarized in Table 1. For each mode where a double Gaussian parametrization is used, the Ξ_c mass is taken as the average of the means of the two Gaussians, weighted by their yields.

Table 1

Signal yields, fitted Ξ_c masses, and reconstruction efficiencies for the Ξ_c decay analyses described in the text.

Decay mode	# of events	mass [MeV/ c^2]	Efficiency [%]
$\Xi_c^+ \rightarrow \Xi^- \pi^+ \pi^+$	3605 ± 279	$2468.6 \pm 0.4 \pm 0.5$	4.55 ± 0.07
$\Xi_c^+ \rightarrow \Lambda K^- \pi^+ \pi^+$	1177 ± 55	$2467.6 \pm 0.2 \pm 0.5$	4.70 ± 0.10
$\Xi_c^+ \rightarrow p K_S^0 K_S^0$	168 ± 27	$2468.6 \pm 0.7 \pm 0.9$	2.45 ± 0.06
$\Xi_c^0 \rightarrow \Xi^- \pi^+$	2979 ± 211	$2471.3 \pm 0.5 \pm 0.8$	7.13 ± 0.14
$\Xi_c^0 \rightarrow \Lambda K^- \pi^+$	3268 ± 276	$2470.0 \pm 0.6 \pm 0.7$	7.31 ± 0.11
$\Xi_c^0 \rightarrow \Lambda K_S^0$	465 ± 37	$2472.2 \pm 0.5 \pm 0.5$	5.36 ± 0.12
$\Xi_c^0 \rightarrow p K^- K^- \pi^+$	1908 ± 62	$2470.9 \pm 0.1 \pm 0.2$	14.00 ± 0.20

4 Ξ_c mass determination

The average masses of the Ξ_c^0 and Ξ_c^+ are determined from the values in Table 1 using the PDG unconstrained averaging algorithm [1, Introduction, p.14–15]:

$$m_{\Xi_c^+} = (2468.1 \pm 0.4 \text{ (stat.} \oplus \text{syst.)}_{-0.2}^{+1.4}) \text{ MeV}/c^2 \quad (\text{PDG : } (2466.3 \pm 1.4) \text{ MeV}/c^2) \quad (8)$$

$$m_{\Xi_c^0} = (2471.0 \pm 0.3 \text{ (stat.} \oplus \text{syst.)}_{-0.2}^{+1.4}) \text{ MeV}/c^2 \quad (\text{PDG : } (2471.8 \pm 1.4) \text{ MeV}/c^2); \quad (9)$$

the first error is the combined statistical and systematic uncertainty, and the second is the uncertainty due to possible biasses in the mass scale (discussed below). We therefore find the $\Xi_c^0 - \Xi_c^+$ mass splitting to be

$$m_{\Xi_c^0} - m_{\Xi_c^+} = (2.9 \pm 0.5) \text{ MeV}/c^2 \quad (\text{PDG} : (5.5 \pm 1.4) \text{ MeV}/c^2). \quad (10)$$

The systematic uncertainty in the mass determination is evaluated as follows. For each mode we vary the order of the polynomial describing the background and the mass range covered by the fit, yielding changes in the fitted mass between 0.1 and 0.5 MeV/ c^2 , depending on the decay. To model imperfect understanding of the signal resolution, we perform fits using signal widths fixed from Monte Carlo, and compare with values where the widths are floated: the mass changes by 0.1–0.5 MeV/ c^2 . Varying the selection criteria, we find a corresponding uncertainty of 0.2–0.8 MeV/ c^2 . To study the possible dependence of the Ξ_c mass on the momentum and decay length of the V^0 's, the mass is estimated in bins of these variables, and an uncertainty of 0.4 MeV/ c^2 is assigned. The total systematic uncertainty is obtained by adding the individual contributions in quadrature.

The possible bias in the overall mass scale is estimated using two approaches. First we reconstruct the following decays, kinematically similar to the ones under study: $\Lambda_c^+ \rightarrow pK^-\pi^+$, $\Lambda_c^+ \rightarrow \Lambda\pi^+\pi^+\pi^-$, $D^0 \rightarrow K_S^0K_S^0$ and $D^+ \rightarrow K^+K_S^0K_S^0$. Comparison of the fitted masses of parent particles with world-average values [1] yields a maximum mass shift of $+1.4 \text{ MeV}/c^2$. Second, using Monte Carlo samples, generated and reconstructed masses are compared for each of the decays (1)–(7), yielding a maximum shift of $\pm 0.2 \text{ MeV}/c^2$. As a result, $^{+1.4}_{-0.2} \text{ MeV}/c^2$ is assigned as a measure of uncertainty in the overall mass scale. Any such shift is assumed to cancel in the mass splitting $m_{\Xi_c^0} - m_{\Xi_c^+}$ (Eq. 10).

5 Ξ_c branching ratios

Branching ratios are evaluated by comparing signal yields for the relevant decays, correcting for reconstruction efficiencies as determined from Monte Carlo (Table 1); branching fractions for the intermediate decays $\Lambda \rightarrow p\pi^-$ and $K_S^0 \rightarrow \pi^+\pi^-$ are taken into account. The modes $\Xi_c^+ \rightarrow \Xi^-\pi^+\pi^+$ and $\Xi_c^0 \rightarrow \Xi^-\pi^+$ are used as references, yielding

$$\frac{\Gamma(\Xi_c^+ \rightarrow \Lambda K^-\pi^+\pi^+)}{\Gamma(\Xi_c^+ \rightarrow \Xi^-\pi^+\pi^+)} = 0.32 \pm 0.03 \pm 0.02 \quad (11)$$

$$\frac{\Gamma(\Xi_c^+ \rightarrow pK_S^0K_S^0)}{\Gamma(\Xi_c^+ \rightarrow \Xi^-\pi^+\pi^+)} = 0.087 \pm 0.016 \pm 0.014 \quad (12)$$

$$\frac{\Gamma(\Xi_c^0 \rightarrow \Lambda K^-\pi^+)}{\Gamma(\Xi_c^0 \rightarrow \Xi^-\pi^+)} = 1.07 \pm 0.12 \pm 0.07 \quad (13)$$

$$\frac{\Gamma(\Xi_c^0 \rightarrow \Lambda K_S^0)}{\Gamma(\Xi_c^0 \rightarrow \Xi^-\pi^+)} = 0.21 \pm 0.02 \pm 0.02 \quad (14)$$

$$\frac{\Gamma(\Xi_c^0 \rightarrow pK^-\pi^+\pi^+)}{\Gamma(\Xi_c^0 \rightarrow \Xi^-\pi^+)} = 0.33 \pm 0.03 \pm 0.03. \quad (15)$$

Table 2

Systematic uncertainties on the signal yields; errors are given in percent (%).

Decay mode	Bkgd shape	Signal width	MC stats	Fragmentation	Total
$\Xi_c^+ \rightarrow \Xi^- \pi^+ \pi^+$	1.2	0.5	1.1	1.0	2.0
$\Xi_c^+ \rightarrow \Lambda K^- \pi^+ \pi^+$	1.4	3.4	2.2	1.0	4.4
$\Xi_c^+ \rightarrow p K_S^0 K_S^0$	1.4	3.0	2.5	1.0	4.3
$\Xi_c^0 \rightarrow \Xi^- \pi^+$	1.6	4.2	2.1	1.0	5.1
$\Xi_c^0 \rightarrow \Lambda K^- \pi^+$	0.8	1.3	1.2	1.0	2.2
$\Xi_c^0 \rightarrow \Lambda K^0$	1.3	3.2	2.5	1.0	4.4
$\Xi_c^0 \rightarrow p K^- K^- \pi^+$	0.3	1.5	1.1	1.0	2.1

Table 3

Systematic uncertainties on the branching ratios; errors are given in percent (%).

Branching ratio	Numerator	Denominator	V^0 recon.	Hadron ID	Total
$\frac{\Gamma(\Xi_c^+ \rightarrow \Lambda K^- \pi^+ \pi^+)}{\Gamma(\Xi_c^+ \rightarrow \Xi^- \pi^+ \pi^+)}$	4.4	2.0	0.0	3.0	5.7
$\frac{\Gamma(\Xi_c^+ \rightarrow p K_S^0 K_S^0)}{\Gamma(\Xi_c^+ \rightarrow \Xi^- \pi^+ \pi^+)}$	4.3	2.0	15.0	0.0	15.7
$\frac{\Gamma(\Xi_c^0 \rightarrow \Lambda K^- \pi^+)}{\Gamma(\Xi_c^0 \rightarrow \Xi^- \pi^+)}$	2.2	5.1	0.0	3.0	6.3
$\frac{\Gamma(\Xi_c^0 \rightarrow \Lambda K_S^0)}{\Gamma(\Xi_c^0 \rightarrow \Xi^- \pi^+)}$	4.4	5.1	5.0	0.0	8.4
$\frac{\Gamma(\Xi_c^0 \rightarrow p K^- K^- \pi^+)}{\Gamma(\Xi_c^0 \rightarrow \Xi^- \pi^+)}$	2.1	5.1	5.0	6.0	9.6

The following sources of systematic error on the efficiency corrected signal yields are considered: uncertainties in the background shape and signal width (evaluated as described in the previous section), uncertainty due to the limited statistics of Monte Carlo samples used to determine efficiencies, and the uncertainty due to charm fragmentation [15]. The latter contribution is estimated using the deviations between the data and Monte Carlo simulation for samples containing D^* mesons, modelled by the fragmentation function of Peterson et al. [16]. The resulting uncertainties are summarized in Table 2; the totals are obtained by adding the individual contributions in quadrature.

When determining the branching ratios, uncertainties due to reconstruction of V^0 's and particle identification of hadrons are taken into account. Based on a comparison of yields for the decays $D^+ \rightarrow K_S^0 \pi^+$ and $D^+ \rightarrow K^- \pi^+ \pi^+$ in data and Monte Carlo, the uncertainty on the efficiency of K_S^0 finding was estimated to be 5.0%. The same value was assigned for Λ finding; in the case (12) we conservatively assume that any such error is anti-correlated with that due to K_S^0 finding, and add the uncertainties linearly. Uncertainties on particle identification efficiency are taken to be 1% for each pion and 2% for each kaon; for the cases (11) and (13), we add these uncertainties linearly. Any error in proton identification efficiencies is assumed to cancel in the ratios (11)–(15). For each branching ratio, the systematic uncertainties from these sources, and from the uncertainties in the yields of the two decay modes (“numerator” and “denominator”; see Table 2), are summarized in Table 3. The total uncertainty is obtained by combining each term in quadrature.

The branching ratio given in Eq. (11) is consistent with the recent FOCUS measurement

$0.28 \pm 0.06 \pm 0.06$ [6], and somewhat lower than the previous CLEO result $0.58 \pm 0.16 \pm 0.07$ [2]; the ratio (15) is compatible with the CLEO result $0.35 \pm 0.06 \pm 0.03$ [4]. The three remaining branching ratios (12, 13 and 14) are measured for the first time. The branching ratio for the decay $\Xi_c^0 \rightarrow \Lambda K_S^0$ is in agreement with the existing theoretical predictions [7,8,9,10]. This measurement is in fact more precise than the current range of theoretical predictions and hence can potentially significantly constrain the above models.

5.1 Resonant substructures in the decay $\Xi_c^0 \rightarrow p K^- K^- \pi^+$

In the $p K^- K^- \pi^+$ final state, a search for the intermediate resonance $\bar{K}^*(892)^0$ is performed by examining the kaon-pion invariant mass distribution for each of the two kaon candidates. This distribution is formed for combinations $p K K \pi$ within three standard deviations of the Ξ_c^0 mass peak, $(2.462\text{--}2.482)$ GeV/c^2 (Fig. 9(a)), and for combinations in the Ξ_c^0 mass sidebands $(2.427\text{--}2.44)$ GeV/c^2 and $(2.50\text{--}2.513)$ GeV/c^2 (Fig. 9(b)). Fig. 10 shows the sideband-subtracted $K\pi$ invariant mass spectrum together with a fit to two components corresponding to resonant $\Xi_c^0 \rightarrow p K^- \bar{K}^*(892)^0$ and non-resonant $\Xi_c^0 \rightarrow p K^- K^- \pi^+$ decays respectively. The shapes of both spectra are determined from Monte Carlo simulation. The decay $\Xi_c^0 \rightarrow p K^- \bar{K}^*(892)^0$ is generated according to a 3-body phase space distribution, and is well-described by a Gaussian and a fourth order polynomial; the non-resonant contribution is parametrized by a fourth order polynomial. In the fit, the only free parameter is the fraction of the resonant component. The fit yields a resonant fraction of $0.51 \pm 0.03 \pm 0.01$, where the systematic error is estimated by varying the parametrization of the two components. The resonant fraction was also recently measured by the CLEO experiment to be 0.39 ± 0.06 (statistical error only). No statistically significant signal for the two-body decay $\Xi_c^0 \rightarrow \Lambda(1520) \bar{K}^*(892)^0$, with the subsequent decays $\Lambda(1520) \rightarrow p K^-$ and $\bar{K}^*(892)^0 \rightarrow K^- \pi^+$, is observed.

6 Conclusions

Seven exclusive decays of the Ξ_c baryon are observed using data collected by the Belle experiment. The masses of charged and neutral states are determined to be $2468.1 \pm 0.4^{+1.4}_{-0.2} \text{ MeV}/c^2$ and $2471.0 \pm 0.3^{+1.4}_{-0.2} \text{ MeV}/c^2$, respectively, and the mass splitting is measured to be $m_{\Xi_c^0} - m_{\Xi_c^+} = (2.9 \pm 0.5) \text{ MeV}/c^2$. Branching ratios relative to the modes $\Xi_c^+ \rightarrow \Xi^- \pi^+ \pi^+$ and $\Xi_c^0 \rightarrow \Xi^- \pi^+$ have also been determined. The branching ratios $\Gamma(\Xi_c^+ \rightarrow \Lambda K \pi \pi)/\Gamma(\Xi_c^+ \rightarrow \Xi \pi \pi) = 0.32 \pm 0.03 \pm 0.02$ and $\Gamma(\Xi_c^0 \rightarrow p K K \pi)/\Gamma(\Xi_c^0 \rightarrow \Xi \pi) = 0.33 \pm 0.03 \pm 0.03$ confirm, with improved precision, previous results of the FOCUS [6] and CLEO [2,4] experiments. The branching ratios $\Gamma(\Xi_c^+ \rightarrow p K_S^0 K_S^0)/\Gamma(\Xi_c^+ \rightarrow \Xi \pi \pi) = 0.087 \pm 0.016 \pm 0.014$, $\Gamma(\Xi_c^0 \rightarrow \Lambda K \pi)/\Gamma(\Xi_c^0 \rightarrow \Xi \pi) = 1.07 \pm 0.12 \pm 0.07$ and $\Gamma(\Xi_c^0 \rightarrow \Lambda K_S^0)/\Gamma(\Xi_c^0 \rightarrow \Xi \pi) = 0.21 \pm 0.02 \pm 0.02$ are measured for the first time. In the decay $\Xi_c \rightarrow p K^- K^- \pi^+$, we find evidence for the decay $p K^- \bar{K}^*(892)^0$ with a fractional yield of $0.51 \pm 0.03 \pm 0.01$. This measurement confirms with higher precision the recent result from the CLEO collaboration [4].

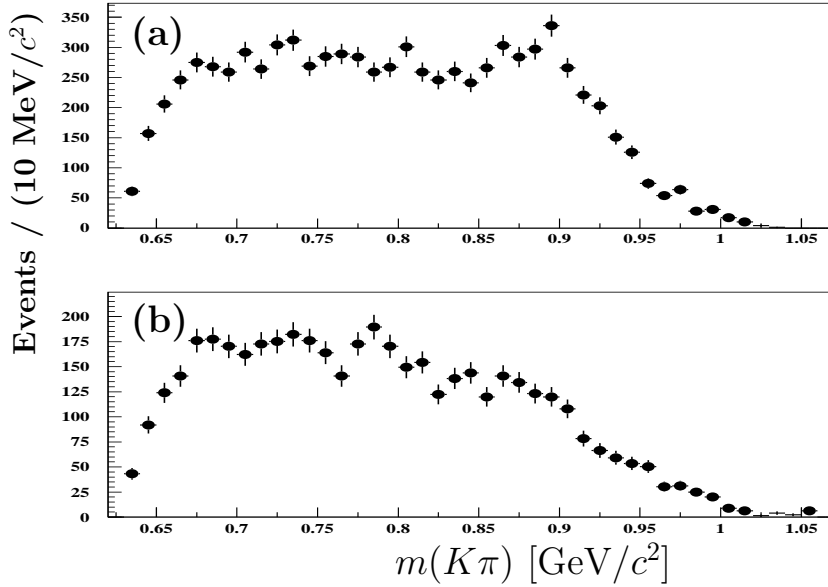


Fig. 9. $\Xi_c^0 \rightarrow pK^-K^-\pi^+$: invariant mass distribution of $K^-\pi^+$ pairs from (a) the Ξ_c^0 peak and (b) the Ξ_c^0 mass sidebands, normalized to the background below the Ξ_c^0 peak.

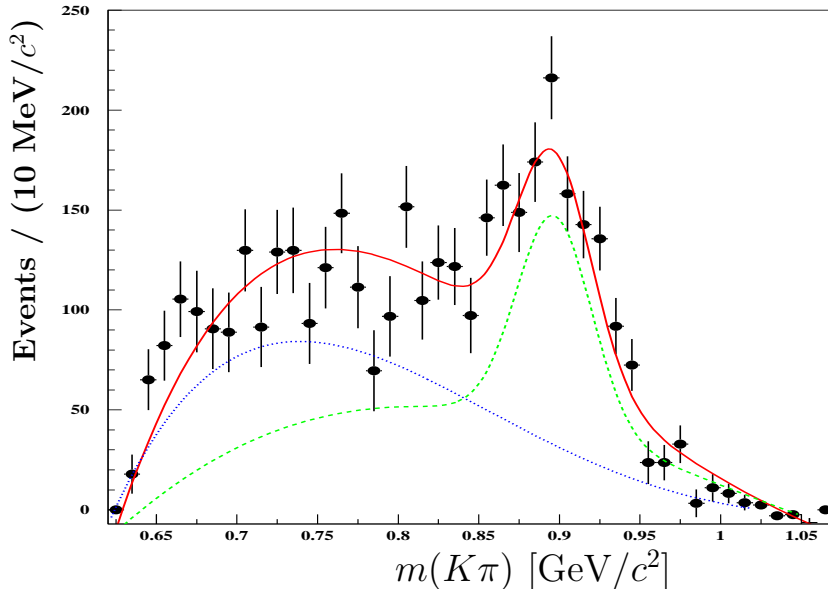


Fig. 10. $\Xi_c^0 \rightarrow pK^-K^-\pi^+$: background subtracted $K^-\pi^+$ invariant mass distribution (points), the fit described in the text (solid curve), the $\Xi_c^0 \rightarrow pK^-\bar{K}^*(892)^0$ component (dashed) and the non-resonant $\Xi_c^0 \rightarrow pK^-K^-\pi^+$ contribution (dotted). The background is modelled using Ξ_c^0 mass sidebands; see Fig. 9.

Acknowledgements

We thank the KEKB group for the excellent operation of the accelerator, the KEK Cryogenics group for the efficient operation of the solenoid, and the KEK computer group and the National Institute of Informatics for valuable computing and Super-SINET network support. We acknowledge support from the Ministry of Education, Culture, Sports, Science, and Technology of Japan and the Japan Society for the Promotion of Science; the Australian Research Council and the Australian Department of Education, Science and Training; the National Science Foundation of China under contract No. 10175071; the Department of Science and Technology of India; the BK21 program of the Ministry of Education of Korea and the CHEP SRC program of the Korea Science and Engineering Foundation; the Polish State Committee for Scientific Research under contract No. 2P03B 01324; the Ministry of Science and Technology of the Russian Federation; the Ministry of Education, Science and Sport of the Republic of Slovenia; the Swiss National Science Foundation; the National Science Council and the Ministry of Education of Taiwan; and the U.S. Department of Energy.

References

- [1] S. Eidelman et al., The Review of Particle Physics, *Phys. Lett. B* 592 (2004) 1.
- [2] T. Bergfeld et al., *Phys. Lett. B* 365 (1996) 431.
- [3] K.W. Edwards et al., (CLEO Collaboration), *Phys. Lett. B* 373 (1996) 261.
- [4] I. Danko et al., (CLEO Collaboration), *Phys. Rev. D* 69 (2004) 052004.
- [5] J.M. Link et al., *Phys. Lett. B* 512 (2001) 277.
- [6] J.M. Link et al., *Phys. Lett. B* 571 (2003) 139.
- [7] B. Desplanques, J.F. Donoghue and B.R. Holstein, *Ann. Phys. (N.Y.)* 124 (1980) 449.
- [8] P. Żenczykowski, *Phys. Rev. D* 40 (1989) 2290.
- [9] P. Żenczykowski, *Phys. Rev. D* 50 (1994) 402.
- [10] K.K. Sharma and R.C. Verma, *Eur. Phys. J. C* 7 (1999) 217.
- [11] S. Kurokawa and E. Kikutani, *Nucl. Instrum. Methods A* 499 (2003) 1, and other papers included in this Volume.
- [12] A. Abashian et al., (Belle Collaboration), *Nucl. Instrum. Methods A* 479 (2002) 117.
- [13] R.E. Kalman, *Trans. Am. Soc. Mech. Eng. D* 82 (1960) 35; R.E. Kalman and R.S. Bucy., *ibid.* 83 (1961) 95.
- [14] T. Lesiak et al., (Crystal Ball Collaboration), *Z. Phys. C* 55 (1992) 33.
- [15] K. Abe et al., (Belle Collaboration), note BELLE-CONF-0335 (2003).
- [16] C. Peterson et al., *Phys. Rev. D* 27 (1983) 105.